

Characterization of the Interfacial Dzyaloshinskii-Moriya Interaction in Pt/Co₂FeAl_{0.5}Si_{0.5} Ultrathin Films by Brillouin Light Scattering

M. Belmeguenai, M. S. Gabor, Y. Roussigné, S.M. Chérif, A. Stashkevich, T. Petrisor, Jr., R. B. Mos and C. Tiusan

Abstract— Brillouin light scattering (BLS) combined with vibrating sample magnetometry (VSM) have been used to investigate the Dzyaloshinskii-Moriya interaction (DMI) in Pt-buffered Co₂FeAl_{0.5}Si_{0.5} ultrathin films of various thicknesses. VSM measurements of the Co₂FeAl_{0.5}Si_{0.5} (CFAS) thickness dependence of the saturation magnetic moment per unit area revealed a magnetization at saturation of 1286 emu/cm³ and 0.31 nm magnetic dead layer. Furthermore, thickest films ($t_{CFAS} > 1$ nm) are in-plane magnetized, while the thinner are perpendicular magnetized. BLS measurements, in the Damon-Eshbach geometry, under an in-plane applied magnetic field revealed the non-reciprocity of the spin waves propagating in opposite directions (Stokes and anti-Stokes lines) due to the Pt induced DMI. Stokes and anti-Stokes lines frequency mismatch varies linearly as function of the spin wave vector allowing the determination of the effective DMI constant. Its thickness dependence leads to determine a value of -0.42 pJ/m for the DMI interface constant, which is significantly lower than that of Pt/Co/AIO_x films. Moreover, BLS measurements revealed that the effective magnetization varies linearly with the effective CFAS thickness due to the perpendicular interface anisotropy, estimated to be 0.49 mJ/m², which reinforces the perpendicular magnetization easy axis.

Index Terms— Dzyaloshinskii-Moriya interaction, Interface anisotropy, Brillouin light scattering, Magnetization dynamics, Spin waves.

I. INTRODUCTION

MAGNETIC exchange interaction is responsible of the homogenous magnetization textures in ferromagnetic

This paragraph of the first footnote will contain the date on which you submitted your paper for review. It will also contain support information, including sponsor and financial support acknowledgment.

“M. S. G., T. P. and R. B. M. acknowledge the financial support of UEFISCDI through PNII-RU-TE-2014-1820—SPINCOD research grant No. 255/01.10.2015.”

M. Belmeguenai, Y. Roussigné, S.M. Chérif and A. Stashkevich are with Laboratoire des sciences des procédés et des matériaux (CNRS-UPR 3407), Université Paris 13, Sorbonne Paris Cité, 99 avenue Jean-Baptiste Clément, 93430 Villetaneuse, France (e-mail: belmeguenai.mohamed@univ-paris13.fr).

M. Gabor, T. Petrisor, Jr., R. B. Mos and C. Tiusan are with the center for Superconductivity, Spintronics and Surface Science, Technical University of Cluj-Napoca, Cluj-Napoca, Romania (e-mail: Mihai.Gabor@phys.utcluj.ro).

materials. This interaction is symmetric leading to collinear orientation of neighboring spins (Heisenberg interaction). In systems with broken symmetry conjugated with spin-orbit coupling, an asymmetric exchange interaction term, known as Dzyaloshinskii-Moriya (DMI) interaction [1, 2] and favoring an orthogonal orientation of spins, can arise. The DMI was used to explain the weak ferromagnetism observed experimentally in antiferromagnetic crystals [3]. The DMI interaction can be bulk or interfacial, when the symmetry of the lattice or that of the interfaces is broken [4], respectively. Therefore, recently a great interest has been growing around magnetic multilayers with interfacial DMI [5-8]. In this case, the needed broken symmetry is given by the interfaces of the material stacks [9, 10], DMI being generated between the ferromagnetic atoms and the heavy atoms directly at the interfaces. The DMI can change the nature of the magnetic domain walls, forcing the appearance of Néel walls [11] and can destabilize the uniformly magnetized states leading to novel chiral magnetic orders such as skyrmions [4, 12]. This has led to novel memory and logic device design, where skyrmions are the information carriers [13]. It is thus interesting for both application and fundamental research to characterize DMI by determine precisely the sign and the value of the effective DMI constant (D_{eff}). Several experimental methods [14-16], largely based on how this interaction alters the properties of domain walls, were performed recently but Brillouin light scattering spectroscopy remains the most direct method for DMI characterization. Moreover, compared to nitrogen-vacancy center microscope [17], which is restricted to small DMI constant values, BLS has no such limit on DMI values.

Co-based full Heusler alloys are of great importance for spintronic applications due to their theoretically predicted half-metallicity [18, 19] and relatively high Curie temperature [20]. Co₂FeAl and Co₂FeSi are ones of the most important Co-based full Heusler alloys due to their low Gilbert damping [21, 22] besides the high Curie temperature. When used as electrodes in MgO (001) based magnetic tunnel junctions (MTJs), they lead to relatively large magnetoresistive ratios [23, 24], increasing the potential applications of these materials. However, band-structure calculations [25] have

indicated that the Fermi level lays near to the top (bottom) of the valence (of the conduction) bands of minority spins for Co_2FeAl (Co_2FeSi). This makes the two compounds prone to finite temperature effects detrimental to half-metallicity. An immediate solution to avoid such effects is the alloying of the two compounds to form $\text{Co}_2\text{FeAl}_{0.5}\text{Si}_{0.5}$ (CFAS), which should virtually move the Fermi level in the middle of the minority gap, increasing the thermal stability of the system.

In this work, we use vibrating sample magnetometry (VSM) combined with Brillouin light scattering (BLS) spectroscopy for a precise determination of the CFAS thickness dependence of the DMI constant and the effective magnetization in Pt/CFAS ultrathin heterostructures.

II. SAMPLES AND SETUPS

CFAS films were grown at room temperature onto thermally oxidized Si substrates using a DC magnetron sputtering system having base pressure lower than 1×10^{-8} Torr. Prior to the deposition of the CFAS films, a Ta (2 nm)/Pt (4 nm) buffer bilayer was grown. Next, CFAS films, of various thicknesses ($t_{\text{CFAS}}=0.7, 0.8, 1$ and 1.2 nm) were sputtered from a stoichiometric target ($\text{Co}_{50\%}\text{Fe}_{25\%}\text{Al}_{12.5\%}\text{Si}_{12.5\%}$) under 1.0 mTorr of Ar. Finally, the films were capped with MgO(1 nm)/Ta(2 nm) bilayer.

Static magnetic characteristics were investigated by vibrating sample magnetometry (VSM). Brillouin light scattering technique [8], in Damon-Eshbach configuration (the magnetic field applied perpendicular to the incidence plane, which allows for probing spin waves propagating along the in-plane direction perpendicular to the applied field), where the DMI effect on the spin waves (SWs) is maximal, has been used to study the SWs non-reciprocity. In this experiment, the SWs, of a wave vector (k_{sw}), in the range $0-20 \mu\text{m}^{-1}$

($k_{\text{sw}} = \frac{4\pi}{\lambda} \sin(\theta_{\text{in}})$, where θ_{in} is the incidence angle), are

probed (in backscattering configuration) by illuminating the sample with a p-polarized incident laser beam having a wavelength $\lambda = 532$ nm. For each angle of incidence, the spectra were obtained after counting photons up to 15 hours (especially for the highest incidence angles where SW peak intensity is weak) to have well-defined spectra where the line position can be determined with accuracy better than 0.2 GHz. A crossed polarizer is placed on the path of the backscattered light to select the SW and removes the phonons. The Stokes (S, negative frequency shift relative to the incident light as a magnon was created) and anti-Stokes (AS, positive frequency shift relative to the incident light as a magnon was absorbed) frequencies, detected simultaneously were then determined from Lorentzian fits to the BLS spectra. All the measurements presented below have been preformed at room temperature.

III. RESULTS AND DISCUSSIONS

For all the studied films, the hysteresis loops were obtained by VSM for both in-plane and perpendicular applied magnetic field, to determine whether CFAS films are spontaneously in-plane or perpendicularly magnetized. Since the saturation field

for the hardest direction [perpendicular (parallel) to the film for in-plane (perpendicularly) magnetized films] can be straightforwardly linked to the perpendicular anisotropy field, only this kind of loops will be presented here. Fig. 1 shows the typical perpendicular applied field magnetization loop for the 1.2 nm thick CFAS film, where a typical hard axis hysteresis loop (Fig. 1) is observed. For an in-plane applied magnetic field, the corresponding hysteresis loop (not shown here) is square suggesting an in-plane easy axis. For each CFAS thickness, the hardest direction hysteresis loop is used to deduce the saturation field (H_a), as shown in figure 2a. This saturation field decreases with increasing CFAS thickness (Fig. 2a), suggesting an interface contribution, that will be precisely evaluated below. Note that negative (positive) H_a values refer to an in-plane (perpendicular to the plane) easy axis. This VSM characterization, revealed that thickest films ($t_{\text{CFAS}} > 1$ nm) are in-plane magnetized (not shown here), while the thinner ones are perpendicularly magnetized, as shown on figure 2a.

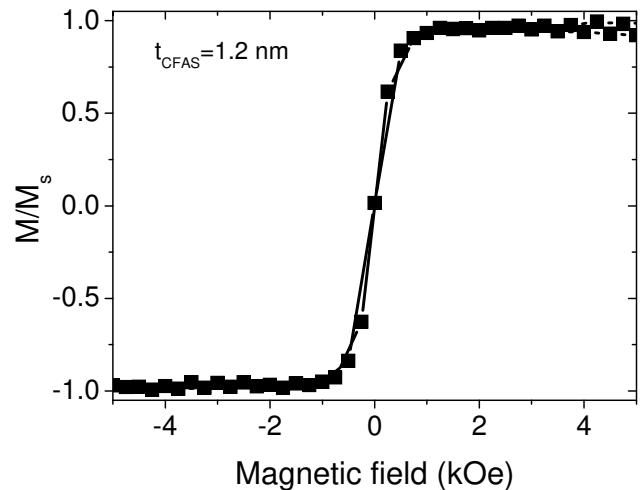


Fig. 1. Perpendicular-to-the-plane applied magnetic field VSM magnetization curves for the Pt/CFAS(1.2 nm)/MgO heterostructure.

The thickness dependence of the saturation magnetic moment per unit area, shown in Fig. 2b was used to determine the magnetization at saturation (M_s) and the extent of the magnetic dead layer (t_d): the slope gives M_s , while the horizontal axis intercept gives t_d . As indicated by figure 2b, the magnetic dead layer thickness (which might form due to intermixing and oxidation of the CFAS during MgO capping layer deposition) is $t_d = 0.31$ nm for this system, and the saturation magnetization is determined to be 1286 emu/cm^3 . This value of M_s is significantly higher than that of the as deposited 30 nm thick CFAS film grown on MgO buffer layer ($M_s = 900-1000 \text{ emu/cm}^3$) [26, 27]. This corresponds to a change in film magnetization of 28% if we consider that $M_s = 1000 \text{ emu/cm}^3$ [27], for MgO/CFAS films. This enhancement of M_s is most probably due the proximity induced magnetization in Pt.

The BLS measurements were performed with the magnetization saturated in the film plane under magnetic fields sufficiently above the saturation fields deduced from the

VSM loops shown in figure 2a. Figure 3 shows the typical BLS spectra at 5 kOe and 7 kOe in-plane applied magnetic field for the 1.2 and 1 nm thick CFAS films for $k_{sw}=15.18 \mu\text{m}^{-1}$ ($\theta_{in}=40^\circ$) and $20.45 \mu\text{m}^{-1}$ ($\theta_{in}=60^\circ$). It reveals the existence of both S and AS spectral lines. Besides the usual intensity asymmetry of these lines due to the coupling mechanism between the light and SWs, a pronounced difference between the frequencies of the S and AS modes ($\Delta F=F_S-F_{AS}$), especially for higher values of k_{sw} , is revealed by the BLS spectra. This frequency mismatch is due to the interfacial DMI as demonstrated previously [7, 8]. It is plotted in figure 4 as a function of k_{sw} , revealing a linear dependence with a slope that changes markedly with CFAS thickness.

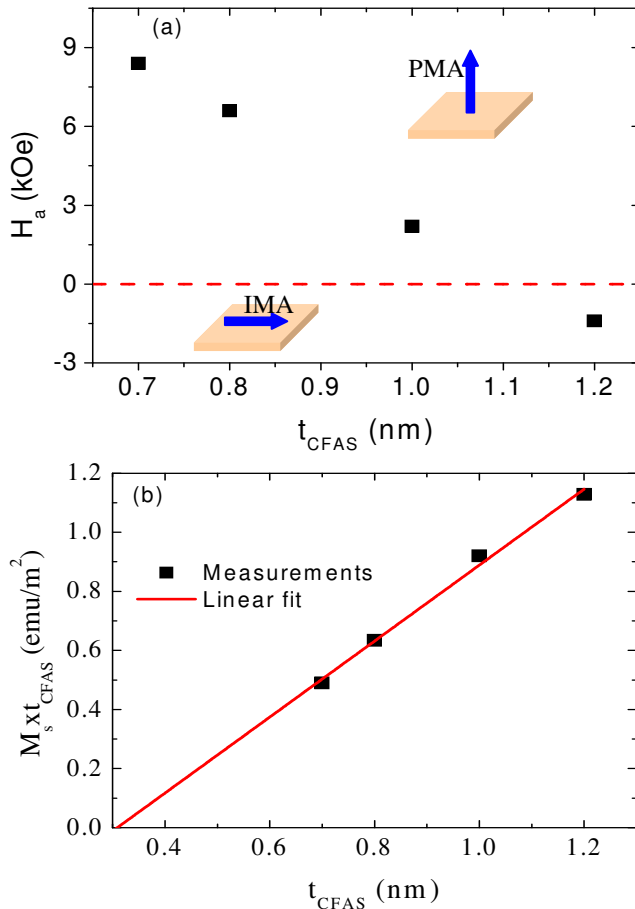


Fig. 2. (Color online) Thickness dependences of (a) the saturation magnetic field in the hard axis plane (b) the saturation magnetic moment per unit area for the CFAS films of various thicknesses (t_{CFAS}). The schematic in (a) refers to CFAS thickness where films have a perpendicular magnetic anisotropy (PMA) and in-plane magnetic anisotropy (IMA). The saturation field is deduced from the hardest direction hysteresis loop.

For all the samples studied here and for positive applied magnetic field, the AS line frequency F_{AS} was found to be always higher than F_S . This means that DMI is negative, i.e., left-handed cycloids are favored. These BLS measurements have been analyzed through the model described in [7, 8], where the k_{sw} dependence of the frequency mismatch induced by DMI is given by:

$$\Delta F = F_S - F_{AS} = \frac{2\gamma}{\pi M_s} D_{eff} k_{sw} = \frac{2\gamma}{\pi M_s} \frac{D_s}{t_{FM}} k_{sw} \quad (1)$$

Here, t_{FM} is the effective ferromagnetic layer thickness ($t_{eff}=t_{FM}-t_d$), $\gamma/2\pi$ is the gyromagnetic ratio and D_s is the interfacial DMI constant. The experimental data were fitted by using the value of M_s determined from VSM and the gyromagnetic ratio, measured previously [28] ($\gamma/2\pi = 29.2$ GHz/T) to determine mainly D_{eff} .

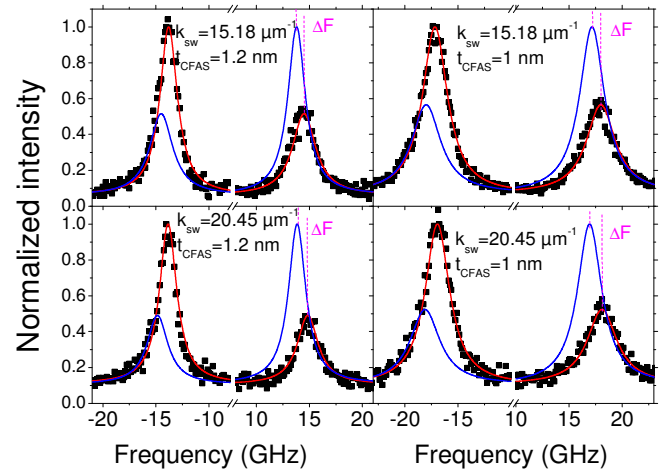


Fig. 3. (Color online) BLS spectra measured for Pt/CFAS(1.2 and 1 nm)/MgO at 5 kOe (for 1.2 nm) and 7 kOe (for 1 nm) in-plane applied magnetic field at two characteristic light incidence angles corresponding to $k_{sw} = 15.18 \mu\text{m}^{-1}$ and $k_{sw} = 20.45 \mu\text{m}^{-1}$. Symbols refer to experimental data and solid lines are fits by Lorentzian. Fits corresponding to negative applied field (blue lines) are presented for clarity and direct comparison of the S and AS frequencies. ΔF is the difference between S and AS frequencies. A crossed polarizer is used to remove phonon lines and select SW scattered light. For clarity, the frequency range -10:10 GHz is removed.

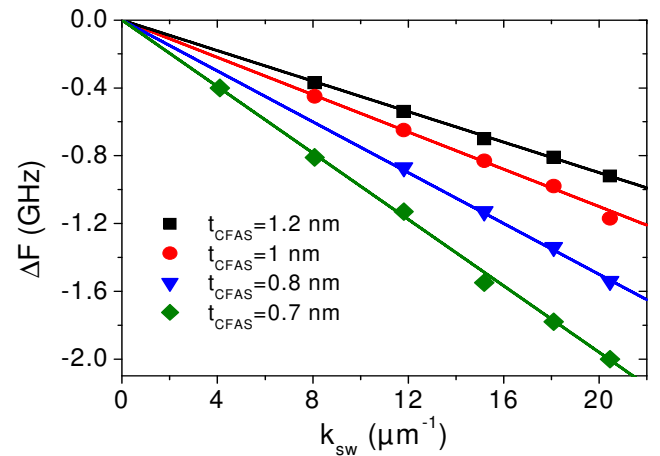


Fig. 4. (Color online) Spin wave vector (k_{sw}) dependence of the experimental frequency difference ΔF (symbols) of Pt/CFAS(t_{CFAS})/MgO systems grown on Si substrates. Solid lines refer to linear fit using equation (1) and magnetic parameter in the text.

Figure 5 shows the obtained values of D_{eff} versus the inverse of the CFAS effective thickness ($1/t_{eff}$). It can be observed that D_{eff} increases (in absolute value) with $1/t_{eff}$ and approaches zero when t_{CFAS} tends to infinity, confirming the interfacial origin of the DMI. The linear fit of the experimental

values of D_{eff} allows determination of a unique value of the surface DMI constant: $D_s = -0.42 \text{ pJm}^{-1}$, which is lower than those of Pt/Co/ AlO_x ($D_s = -1.7 \text{ pJm}^{-1}$) [8] and Pt/CoFeB/MgO ($D_s = 0.8 \text{ pJm}^{-1}$) [29]. CFAS films being Heusler alloys are subject of some degree of chemical disorder, which strongly influences many of their physical properties and probably also the DMI. Very thin and as-grown CFAS films have usually the A2 structure, corresponding to a complete disorder between all atoms Co, Fe and Si-Al. Therefore, within the CFAS thickness range presented in this paper, all films show mostly the same disordered A2 structure, which may explain the smaller DMI constant in Pt/CFAS compared to Pt/Co and Pt/CoFeB. Moreover, as shown by Jang et al. [30], based on numerical studies, the interfacial DMI decreases the thermal energy barrier while it increases the switching current and thus DMI should be minimized for perpendicular spin transfer torque memory applications. This again increases the potential application of such Heusler alloys. However, higher DMI values are needed for stabilizing magnetic Skyrmions [31], interesting for achieving high information density in magnetic data storage and other spintronic devices.

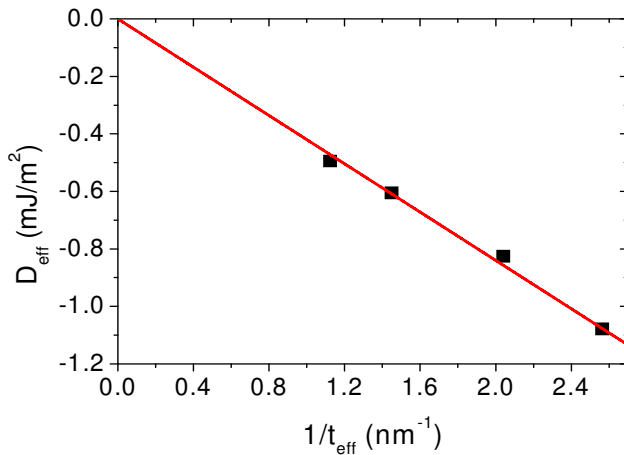


Fig. 5. (Colour online) Thickness dependence of the effective DMI constants extracted from fits of Fig. 4 using equation (1). Symbols refer to the experimental data and solid line is the linear fit.

We have also been interested by the investigation of the perpendicular anisotropy in Pt/CFAS/MgO systems using the BLS measurements. In figure 6a are plotted the average value of the S and AS frequencies $[f_0 = (F_S + F_{AS})/2]$ and Δf versus the in-plane applied magnetic field for the 1.2 nm and 1 nm thick CFAS films at $k_{sw} = 8.08 \mu\text{m}^{-1}$ ($\theta_{in} = 20^\circ$) and $15.18 \mu\text{m}^{-1}$ ($\theta_{in} = 40^\circ$), respectively. It is worth noting that BLS measurements of Δf as a function the in-plane applied magnetic field [see the inset of Fig. 6a for 1.2 nm and 1 nm thick CFAS films] reveal that Δf is independent of the applied field, as expected from the model mentioned above in equation (1). The experimental field dependence of f_0 has been fitted using equation (1) of reference [8] to deduce the effective magnetization ($4\pi M_{eff} = 4\pi M_s - 2K_{\perp}/M_s$, where K_{\perp} is the perpendicular anisotropy constant). The thickness dependence of M_{eff} is shown in figure 6b, where it can be seen that M_{eff} follows a linear variation. We conclude that the perpendicular effective

magnetic anisotropy can be described by a volume (K_v) and an interface (characterized by the constant K_s) contributions, as given by equation (2).

$$K_{\perp} = K_v + \frac{K_s}{t_{eff}} \quad (2)$$

The linear fit of the M_{eff} measurements versus $1/t_{eff}$, combined with equation (2), allows for the determination of the perpendicular surface ($K_s = 0.49 \text{ mJ/m}^2$) and volume ($K_v = 0.48 \times 10^6 \text{ J/m}^3$) anisotropy constants from the slope and y-intercept, respectively. Both K_s and K_v are positive reinforcing the perpendicular magnetization easy axis. The K_s value is comparable to that of Pt/Co/ AlO_x [32].

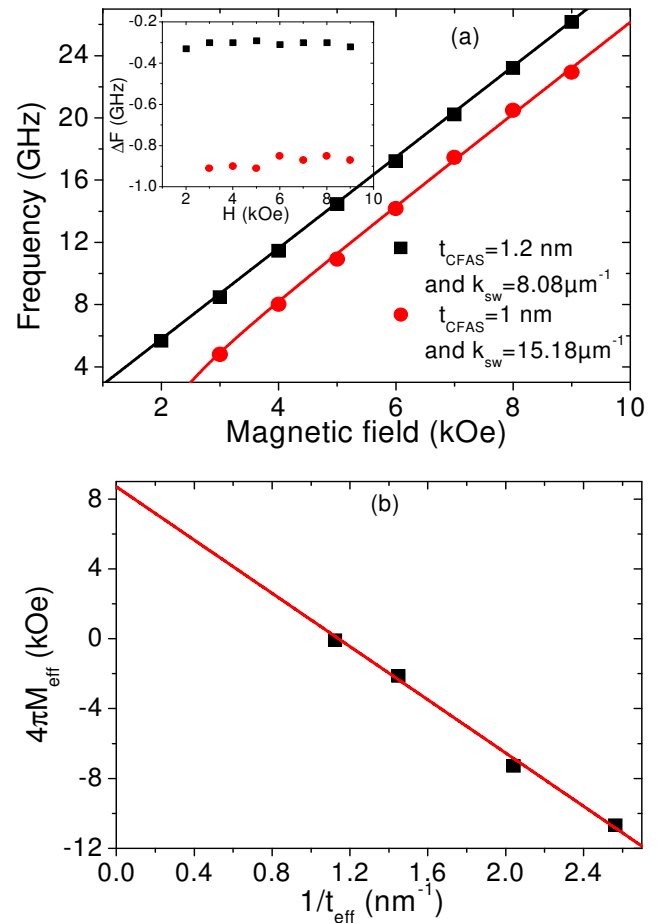


Fig. 6. (Colour online) Field dependence of the mean frequency of S and AS lines ($(F_S + F_{AS})/2$) for the 1.2 nm (black curves measured at $k_{sw} = 8.08 \mu\text{m}^{-1}$) and 1 nm (red curves measured at $15.18 \mu\text{m}^{-1}$) thick CFAS films. Symbols refer to the experimental data and solid lines are fits using equation (1) of reference [8]. The inset shows the measured dependence of Δf versus the applied magnetic field in the case of the $t_{CFAS} = 1.2 \text{ nm}$ and 1 nm sample at a fixed wave vector values $k_{sw} = 8.08 \mu\text{m}^{-1}$ and $k_{sw} = 15.18 \mu\text{m}^{-1}$. (b) Thickness dependence of the effective magnetization extracted from fits of similar measurements of Fig. 6a. Symbols refer to the experimental data and solid line is the linear fit.

IV. CONCLUSION

The thickness dependence of the DMI constant has been investigated in Pt/CFAS/MgO systems via Brillouin light scattering. We proved that this scheme is simple, efficient,

reliable and straightforward since few parameters are required for the experimental data fit. The obtained results demonstrate lower DMI constants in Pt/CFAS/MgO compared to Pt/Co structure reinforcing the interest of such Heusler alloys for perpendicular spin transfer torque memory applications. Moreover, we demonstrate the possibility of perpendicular magnetization of the ultrathin CFAS films due the existence of both volume and interface contribution.

REFERENCES

- [1] I. E. Dzyaloshinskii, "Thermodynamical theory of "weak" ferromagnetism in antiferromagnetic substances", *Sov. Phys. JETP* 5, 1259 (1957).
- [2] T. Moriya, "Anisotropic superexchange interaction and weak ferromagnetism", *Phys. Rev.* 120, 91 (1960).
- [3] I. Dzyaloshinsky, "A thermodynamic theory of "weak" ferromagnetism of antiferromagnetics", *J. Phys. Chem. Solids* 4, 241 (1958).
- [4] A. Fert, V. Cros and J. Sampaio, "Skyrmions on the track", *Nat. Nanotechnol.* 8, 152 (2013).
- [5] S-G. Je, D-H. Kim, S-C. Yoo, B-C. Min, K-J. Lee, and S-B. Choe, "Asymmetric magnetic domain-wall motion by the Dzyaloshinskii-Moriya interaction", *Phys. Rev. B* 88, 214401 (2013).
- [6] A. Hrabec, N. A. Porter, A. Wells, M. J. Benitez, G. Burnell, S. McVitie, D. McGrouther, T. A. Moore, and C. H. Marrows, "Measuring and tailoring the Dzyaloshinskii-Moriya interaction in perpendicularly magnetized thin films", *Phys. Rev. B* 90, 020402(R) (2014).
- [7] K. Di, V. L. Zhang, H. S. Lim, S. C. Ng, M. H. Kuok, J. Yu, J. Yoon, X. Qiu, and H. Yang, "Direct observation of the Dzyaloshinskii-Moriya interaction in a Pt/Co/Ni film", *Phys. Rev. Lett.* 114, 047201 (2015).
- [8] M. Belmeguenai, J-P. Adam, Y. Roussigné, S. Eimer, T. Devolder, J-V. Kim, S. M. Chérif, A. Stashkevich, and A. Thiaville, "Interfacial Dzyaloshinskii-Moriya interaction in perpendicularly magnetized Pt/Co/AlOx ultrathin films measured by Brillouin light spectroscopy", *Phys. Rev. B* 91, 180405(R) (2015).
- [9] H. Yang, A. Thiaville, S. Rohart, A. Fert, and M. Chshiev, "Anatomy of Dzyaloshinskii-Moriya interaction at Co/Pt Interfaces", *Phys. Rev. Lett.* 115, 267210 (2015).
- [10] A. Crepieux and C. Lacroix, "Dzyaloshinsky-Moriya interactions induced by symmetry breaking at a surface", *J. Magn. Magn. Mater.* 182, 341 (1998).
- [11] M. Heide, G. Bihlmayer, and S. Blügel, "Dzyaloshinskii-Moriya interaction accounting for the orientation of magnetic domains in ultrathin films: Fe/W(110)", *Phys. Rev. B* 78, 140403(R) (2008).
- [12] N. Nagaosa and Y. Tokura, "Topological properties and dynamics of magnetic skyrmions", *Nat. Nanotechnol.* 8, 899 (2013).
- [13] X. Zhang, M. Ezawa, and Y. Zhou, "Magnetic skyrmion logic gates: conversion, duplication and merging of skyrmions", *Sci. Rep.* 5, 9400 (2015).
- [14] S. Pizzini, J. Vogel, S. Rohart, L. D. Buda-Prejbeanu, E. Jué, O. Boulle, I. M. Miron, C. K. Safeer, S. Auffret, G. Gaudin, and A. Thiaville, "Chirality-induced asymmetric magnetic nucleation in Pt/Co/AlOx ultrathin microstructures", *Phys. Rev. Lett.* 113, 047203 (2014).
- [15] S. Emori, E. Martinez, K.-J. Lee, H.-W. Lee, U. Bauer, S.-M. Ahn, P. Agrawal, D. C. Bono, and G. S. D. Beach, "Spin Hall torque magnetometry of Dzyaloshinskii domain walls", *Phys. Rev. B* 90, 184427 (2014).
- [16] [1] J. Torrejon, J. Kim, J. Sinha, S. Mitani, M. Hayashi, M. Yamanouchi, and H. Ohno, "Interface control of the magnetic chirality in CoFeB/MgO heterostructures with heavy-metal underlayers", *Nat. Commun.* 5, 4655 (2014).
- [17] I. Gross, L. J. Martínez, J.-P. Tetienne, T. Hingant, J.-F. Roch, K. Garcia, R. Soucaille, J. P. Adam, J.-V. Kim, S. Rohart, A. Thiaville, J. Torrejon, M. Hayashi, and V. Jacques, "Direct measurement of interfacial Dzyaloshinskii-Moriya interaction in X[CoFeB]MgO heterostructures with a scanning NV magnetometer (X=Ta,TaN, and W)", *Phys. Rev. B* 94, 064413 (2016).
- [18] I. Galanakis, P. H. Dederichs, and N. Papanikolaou, "Slater-Pauling behavior and origin of the half-metallicity of the full-Heusler alloys", *Phys. Rev. B* 66, 174429 (2002).
- [19] S. Picozzi, A. Continenza, and A. J. Freeman, "Co₂MnX (X=Si, Ge, Sn) Heusler compounds: An ab initio study of their structural, electronic, and magnetic properties at zero and elevated pressure", *Phys. Rev. B* 66, 094421 (2002).
- [20] S. Trudel, G. Wolf, J. Hamrle, B. Hillebrands, P. Klaer, M. Kallmayer, H.-J. Elmers, H. Sukegawa, W. Wang, and K. Inomata, "Effect of annealing on Co₂FeAl_{0.5}Si_{0.5} thin films: A magneto-optical and x-ray absorption study", *Phys. Rev. B* 83, 104412 (2011).
- [21] M. Belmeguenai, H. Tuzcuoglu, M. S. Gabor, T. Petrisor, C. Tiusan, D. Berling, F. Zighem, T. Chauveau, S. M. Chérif, and P. Moch, "Co₂FeAl thin films grown on MgO substrates: Correlation between static, dynamic, and structural properties", *Phys. Rev. B* 87, 184431 (2013).
- [22] M. Oogane, R. Yilgin, M. Shinano, S. Yakata, Y. Sakuraba, Y. Ando, and T. Miyazaki, "Magnetic damping constant of Co₂FeSi Heusler alloy thin film", *J. Appl. Phys.* 101, 09J501 (2007).
- [23] W. Wang, H. Sukegawa, R. Shan, S. Mitani, and K. Inomata, "Giant tunneling magnetoresistance up to 330% at room temperature in sputter deposited Co₂FeAl/MgO/CoFe magnetic tunnel junctions", *Appl. Phys. Lett.* 95, 182502 (2009).
- [24] Z. Gercsi, A. Rajanikanth, Y. K. Takahashi, K. Hono, M. Kikuchi, N. Tezuka, and K. Inomata, "Spin polarization of Co₂FeSi full-Heusler alloy and tunneling magnetoresistance of its magnetic tunneling junctions", *Appl. Phys. Lett.* 89, 082512 (2006).
- [25] G. H. Fecher and C. Felser, "Substituting the main group element in cobalt-iron based Heusler alloys: Co₂FeAl_{1-x}Si_x", *J. Phys. D* 40, 1582 (2007).
- [26] W. Wang, H. Sukegawa, R. Shan, and K. Inomata, "Large tunnel magnetoresistance in Co₂FeAl_{0.5}Si_{0.5}/MgO/Co₂FeAl_{0.5}Si_{0.5} magnetic tunnel junctions prepared on thermally oxidized Si substrates with MgO buffer", *Appl. Phys. Lett.* 93, 182504 (2008).
- [27] W. Wang, H. Sukegawa, R. Shan, T. Furubayashi, and K. Inomata, "Preparation and characterization of highly L₂₁-ordered full-Heusler alloy Co₂FeAl_{0.5}Si_{0.5} thin films for spintronics device applications", *Appl. Phys. Lett.* 92, 221912 (2008).
- [28] M. S. Gabor, M. Belmeguenai, T. Petrisor, Jr., C. Ulhaq-Bouillet, S. Colis, and C. Tiusan, "Correlations between structural, electronic transport, and magnetic properties of Co₂FeAl_{0.5}Si_{0.5} Heusler alloy epitaxial thin films", *Phys. Rev. B* 92, 054433 (2015).
- [29] K. Di, V. L. Zhang, H. S. Lim, S. C. Ng, M. H. Kuok, X. Qiu, and H. Yang, "Asymmetric spin-wave dispersion due to Dzyaloshinskii-Moriya interaction in an ultrathin Pt/CoFeB film", *Appl. Phys. Lett.* 106, 052403 (2015).
- [30] P.-H. Jang, K. Song, S.-J. Lee, S.-W. Lee, and K.-J. Lee, "Detrimental effect of interfacial Dzyaloshinskii-Moriya interaction on perpendicular spin-transfer-torque magnetic random access memory", *Appl. Phys. Lett.* 107, 202401 (2015).
- [31] C. Moreau-Luchaire, C. Moutafis, N. Reyren, J. Sampaio, C. A. F. Vaz, N. Van Horne, K. Bouzehouane, K. Garcia, C. Deranlot, P. Warnicke, P. Wohlhüter, J.-M. George, M. Weigand, J. Raabe, V. Cros, and A. Fert, "Additive interfacial chiral interaction in multilayers for stabilization of small individual skyrmions at room temperature", *Nature Nanotechnology* 11, 444 (2016).
- [32] N-H. Kim, D-S. Han, J. Jung, J. Cho, J-S. Kim, Henk J. M. Swagten, and Ch-Y. You, "Improvement of the interfacial Dzyaloshinskii-Moriya interaction by introducing a Ta buffer layer", *Appl. Phys. Lett.* 107, 142408 (2015).